



# STUDY OF NANOSTRUCTURE SYNTHESIS FOR TRIBOLOGICAL PHOTOCATALYTIC

Ambala Sudarshan, Dr. Chaudhari Kishor Gopalrao  
Department of Physics, College- Malwanchal University, Indore

2662

## ABSTRACT

Research into nanoparticles has progressed, leading to an uptick in their use in a variety of fields, including medicine. In medicine, for instance, nanoparticles have garnered interest because of their potential to increase drug delivery, efficiency, and safety. In biological and cell imaging applications, where the absorption and scattering characteristics and optical resonance wavelength of NPs like Au and Ag can be determined, NPs are chosen to create efficient contrast.

Magnetite ( $Fe_3O_4$ ), one type of magnetic nanoparticles, has recently found use in the medical field. Finding the proper chemical composition for super magnetic iron oxide nanoparticles has helped researchers advance MRI, medication delivery, cell separation, and immunoassays. NPs need to be highly magnetized, homogenous in size, smaller than 100 nm in size, and used in these applications. Various dyes, enzymes, radioactive chemicals, and AuNPs can be used to label antibodies for tissue identification.

Light scattering and absorption properties of semiconductor and metal nanoparticles hold great promise for cancer detection and therapy. The nanoparticles of gold can be used to specifically target cancerous tissues by converting the electromagnetic energy from an electromagnetic field into heat. In a study on the use of Au-silica NPs to treat prostate cancer, gold-silica nanoshells (GSNs) were used in conjunction with MRI-ultrasound imaging to destroy prostate tumor cells selectively. These NPs absorbed NIR light, leading to hyperthermia and the eventual death of tumor cells.

DOI Number: 10.14704/nq.2022.20.13.NQ88333      Neuro Quantology 2022; 20(13):2662-2674

## INTRODUCTION

These nanostructures have unique functional features that set them apart from their bulk counterparts. The benefits of nanoparticles, then, hinge on scientists' capacity to tailor the geometries of materials at ever-shrinking dimensions to produce the desired effects, thereby bolstering the expanding scientific canon. It is possible to manufacture materials with tailored properties, such as those with desirable electrical, physical, optical, and imaging characteristics.

In the textile industry, nanoparticles are added to or used to treat fabric surfaces, improving ballistic protection properties and lowering the likelihood of wrinkles and bacterial growth. The emergence of nanomaterials is paving the way for the development of washable, resilient "smart fabrics" that incorporate nanoscale sensors and electronic components to perform tasks like

health tracking, solar energy capture, and energy harvesting through movement.

Technology such as smartphones, fitness trackers, and smart thermostats are all examples of consumer goods that make use of nanoparticles. Nanotechnology is expected to revolutionize many industries, including the production and storage of food. The use of RET (resonant energy transfer) systems that include nanoparticles of noble metals is expanding in the optical and materials sciences. For the purpose of incorporating NPs into foreseeable consumer goods.

## Characterization of Nanomaterials

Nanomaterials can be classified as either inorganic (non-carbon) or organic (hydrocarbon) based on their chemical composition. Inorganic nanomaterials include metal-based NPs, metal oxide/hydroxide NPs, and transition metal chalcogenide or TMC NPs, whereas organic nanomaterials include carbon-



and hydrogen-containing NPs including nanospheres, nanocapsules, micelles, liposomes, dendrimers, hybrid NPs, and carbon-based NPs. There are several varieties of carbon-based nanomaterials, including but not limited to graphene, carbon nanotubes, and fullerenes.

## Inorganic Nanomaterials

### ➤ Metal NPs

Metal nanoparticles (metal NPs) are single-element nanomaterials. They may exist as clusters or as single atoms. Particles may also exist in nanocluster forms, such as Au<sub>8</sub>, Au<sub>11</sub>, Au<sub>13</sub>, Au<sub>18</sub>, Au<sub>25</sub>, Au<sub>38</sub>, and Au<sub>55</sub>, as well as in neutral states like Au(0), Au, Ag(0), and Ag, with particular electronic transitions. These luminous NPs, which display luminescent patterns and fluorescence resonance energy transfer, are employed for biolabelling. Ag, Cu, Au, Pt, Pd, Re, Zn, Ru, Co, Cd, Al, and Pb are often produced NPs; Fe and Ni are explosive and extremely reactive. Additionally, bimetallic NPs (such as Pt-Pd, Cu-Ni) fall under the umbrella of metal NPs and are often seen in core-shell and alloy forms. Better and more effective than single-metal NPs are bimetallic NPs.

### ➤ Metal Oxide NPs

Because anionic oxygen is present, when an electronegative oxygen and an electropositive metal react, oxides with polar surfaces are produced. The majority of organic solvents cannot dissolve them. They are quite common and occur naturally. They have tunable band gaps and edges, are chemically stable, and are good heat- and electricity-conductors. They are used in insulators, semiconductors, and even superconductors. Some adaptable metal oxides that can be readily modified by doping to improve their hetero-structures, characteristics, and efficiency are Al<sub>2</sub>O<sub>3</sub>, Fe<sub>3</sub>O<sub>4</sub>, TiO<sub>2</sub>, Fe<sub>2</sub>O<sub>3</sub>, ZnO, CeO<sub>2</sub>, and SiO<sub>2</sub>. Because of their specialised structure and composition, layered metal hydroxides have adjustable characteristics. They may be found in one of two ways: (1) as hydroxides with neutral layers and no intercalation, and (2) as hydroxides with cationic layers and intercalation. They have strong ion exchange capacity, large surface area, and great thermal stability. Supercapacitors, catalysis, fuel cells, sensors, flame retardants, and pollution

removal systems are only a few applications for them.

### ➤ Metal Chalcogenides (MCs)

Metal chalcogenides are a class of inorganic nanomaterials that consist of a metal and one of four different chalcogen anion types: O<sup>2-</sup>, Te<sup>2-</sup>, Se<sup>2-</sup>, and S<sup>2-</sup>. Nanocompounds are typically limited to selenide, telluride, and sulfide rather than polonium or oxide nanocompounds due to the polar behavior of gaseous and non-metallic oxygen and highly metallic polonium. Numerous transition metals, including MoS<sub>2</sub>, and post-transition series metal chalcogenides, such as GaS, have been studied extensively since the 1960s due to their excitonic and electronic absorption and quasi-2D behavior. It's worth noting that symmetry-protected topological states can be found in the tellurides and bismuth selenides. The chemical formula for layered transition metal dichalcogenides (TMDs) is MX<sub>2</sub>. These materials have van der Waals layer conformations. Each monolayer has a covalently bound X-M-X sandwich structure. Since elements can exist in a wide range of polymorphs with different coordinations and polytypes with different stacking orders, at least forty different kinds of layered TMDs can be made from them. One can further categorize the layered TMDs as follows: 1T, or octahedral coordinated, monolayer unit cell trigonal and distorted 1T'; 2H, or trigonal prismatic coordinated bilayer unit cell, hexagonal; 3R, or trigonal prismatic coordinated trilayer unit cell, hexagonal; and. In contrast to the metallic nature of all other phases, 2H nanosheets are semiconducting. MoS<sub>2</sub> is a typical TMD group 6 nanomaterial due to its catalytic, adsorption, and lubricating properties.

## Organic Nanomaterials

As shown, organic NPs include micelles, liposomes, ferritin, hybrid molecules, and dendrimers. They are safe, biodegradable, and environmentally friendly. Micelles and liposomes with hollow cores are light- and heat-sensitive. Due to their excellent biocompatibility, stability, load capacity, and surface shape, they are excellent drug delivery agents. Liposomes' phospholipid vesicles, which vary in size from 50 to 100 nm, naturally only contain lipidic substances, while unilamellar liposomes have a diameter of 100 to 800 nm. The spherical structures of liposomes are formed by



amphiphilic chemicals, which are typically fully biodegradable, biocompatible, adaptable, non-immunogenic, have excellent trapping efficiency, and are non-toxic. Amphiphilic substances, such as polymers or lipids, are found in micelle NPs and vary in size from 10 to 100 nm. They have a high biostability and drug trapping capability.

## CLASSIFICATION OF NANOSTRUCTURES

Several different types of nanostructures, such as nanotubes, nanofibers, nanorods, etc., have been reported in the scientific literature, as we saw in the previous section. In this part, we elaborate on this idea by describing the salient features of several types of these nanostructures. In particular, we aim to define the various nanostructures, explain how they are made, and identify the critical factors (such as pH, surfactant use, and production temperature) that govern their creation and potential uses. Not only are the most common techniques for creating such nanostructures highlighted where applicable, but also any other techniques that bear importance.

### Nanospheres

The creation of spherical particles with average diameters in the nanometer range is at the heart of the nanosphere innovation. Due to their nanoscale size and ability to encapsulate and release pharmacological or active compounds, they serve as ideal carriers for various applications. In order to create nanospheres, a common method is to use the mini-emulsion technique (Figure 1), in which a precursor is dissolved into an organic solvent (oil phase). This component is incorporated into a water-based aqueous solution that also includes a surfactant or stabilizer. After further homogenization with a sonicator, nanospheres are collected via ultracentrifugation. To ensure optimal fusion of the active molecules and medications into the nanospheres, they can be loaded in either an aqueous or an oil phase. Nanospheres can be characterized by their morphology, size, and drug encapsulation using various electron microscopy techniques. The diameter (size) and shape of the nanospheres can be adjusted by adjusting the concentration of the precursors, the ratio of the precursor surfactant or stabilizer, and the speed of the homogenizer.

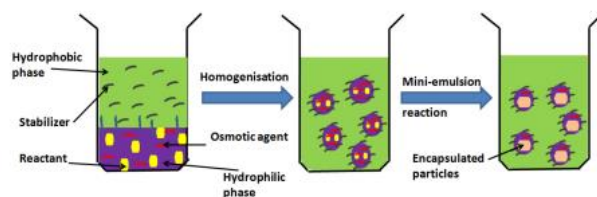


Figure 1. A schematic of a mini-emulsion process

Depositions of nanospheres on colloidal crystals are typically prepared using nanosphere lithography (NSL), another prominent technique. These allow for low-cost, high-throughput processing, a sizable fabrication area, and a wide variety of materials, all while facilitating the creation of a wide range of nanostructures on planar and non-planar substrates. The advantages of both top-down and bottom-up approaches are brought together in this method. There are two phases to the process. The first is to employ prefabricated silica or latex nanospheres with solid backings as the lithography substrate. Substrates treated with a chemical to increase their hydrophilicity are used in the second stage. These substrates are covered with a suspension comprising monodisperse colloids (such as polystyrene). For the purpose of designing new nanospheres, a monolayer or bilayer of hexagonal close-packed (HCP) material is first formed, allowed to dry, and then framed to form a colloidal crystal mask (CCM). After the mask is stripped off or sonicated away in the right solvent, an ordered array of nanodots is left behind on the substrate. To crystallize the sample or to cause a crystallographic phase transition, annealing is sometimes required. Colloidal lithography, also known as characteristic lithography, is another name for nanosphere lithography.

Fischer and Zingsheim were among the first to report the formation of a stable monolayer on a glass substrate in 1981. They used a colloidal deposition method to create nanospheres with a particle diameter of >300 nm and then dried them. This method was given its current name, nanosphere lithography, by researchers Hulteen and Van Duyne in the 1990s. By employing this method, Hulteen and Van Duyne were able to create a double layer (DL), which encourages the arrangement of tiny particles in relation to the tiny openings that remain in a closed, compressed structure. So, research into the

plasmon reverberation properties of metallic materials was conducted with the intent of developing surface-enhanced Raman spectroscopy-based biosensors. Furthermore, some groups have theoretically examined the behavior of colloidal suspensions to comprehend their stability and also the mask's arrangement system. The ability of nanosphere lithography to fabricate a wide variety of one-, two-, and three-dimensional nanostructures has attracted attention over the years. It is important to accurately evaluate the most practical approach to producing nanospheres using this method with the desired properties for use in biomedical applications. Materials should be biocompatible and biodegradable for best results. However, the goals of the design, the resolution of the patterning, the cost of fabrication, the variety of materials available, the throughput, the complexity, and the capacity for mass production are all factors to be taken into account when deciding on a manufacturing strategy. Regardless, mold costs for producing nanospheres rise precipitously as component sizes decrease and mold surface areas grow. Scientists' ultimate goal is to increase industrial production. Therefore, when deciding the strategy to create NPs for biomedical applications, it is important to take the ability to scale-up into account. Adjusting the conditions for mass production is difficult even though industries have adopted the above strategies to manufacture various NPs.

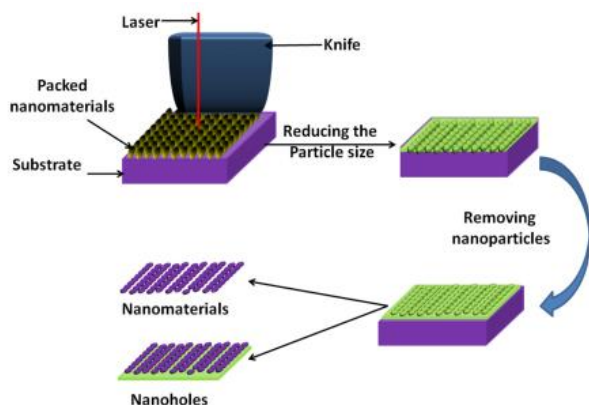


Figure 2. Schematic diagram for nanosphere lithography

### Nanorods

Nanorods (NPs) are characterized by having dimensions less than 100 nm and two faces with

an aspect ratio of 3, 4, or 5. Nanorods have superior general characteristics to those of spherical particles. This is because increasing the aspect ratio of the NPs causes the excitation of surface plasmons to increase. It has been shown that light-activated, on-demand pulsatile discharge resources carrying exceptionally enhanced treatments can be provided via flexible drug delivery systems using nanoporous layers that comprise gold nanorods and dendrimers. Both the static and fluidic devices' drug release rates are correlated with the near IR laser's temperature increase and luminous energy. In vitro evaluations have also shown the biocompatibility of this on-demand control platform. This demonstrates the adaptability of on-demand slow medication delivery in specialized treatment regimes, as each medicine has shown strikingly different reactions for improvements in the excitation state compared to the non-excitation condition. Because of the changes to the plasma drug profiles brought about by these nanocarriers, therapeutic efficacy will be increased while adverse effects are decreased. However, the resistance of neighboring typical tissues limits hyperthermia's efficacy as a treatment for classical disease. Gold nanorods (NRs) administered parenterally as a photosensitizer improve the efficacy of hyperthermia treatment without damaging normal tissues.

Table 1. Example references (Refs.) featuring the impacts of typical physico-chemical properties of nanoparticles (NPs) on the uptake of cells

Physicochemical Properties	Parameter	NPs	Uptake Mechanism	Effects of Important Characteristics
Surface charge	Positive, negative and neutral	poly(ethylene glycol)-block-poly(lactic acid) PEG-b-PLA	Clathrin- and caveolin-mediated endocytosis	Positive charge improves uptake, transport and distribution
Size	5-100 nm	Ag	Clathrin-mediated endocytosis	Higher uptake of larger NPs; lower cross-plasma membrane becomes faster
Shape	Nanospheres and nanostars	Small interfering RNA-conjugated Au	Endocytosis	Larger spheres (50 nm) and stars (40 nm) show higher uptake

### Nanostars

Several nanostructures in the shape of a star made of metal have been produced for use in medicine. The technique in this case entails fabricating a biocompatible gold nanoparticle star (GNS) without the use of the toxic surfactants typically necessary for GNS production. Several of



the sharp edges found in AGNS function like lightning rods, greatly amplifying the local electromagnetic field. When compared to alternative gold nanoparticle geometries, the structure improves grounded surface-enhanced Raman scattering (SERS), two-photon activity cross-segment, and photothermal transformation efficiency. Nanoparticle penetration through the blood-membrane barrier in brain tumors was also studied using GNSs. Although many aspects of GNSs have been studied, their in vivo biodistribution, tumour uptake, intra-tumoral dissemination, and the possibility of in vivo computed tomography (CT) imaging, surface-enhanced Raman scattering (SERS) location, and tumour proliferating trichilemmal tumour (PTT) removal have yet to be thoroughly investigated. The multifunctional GNS test was used for imaging and therapy in this in vivo study. The effect of NP size and infusion volume on biodistribution and intra-tumoral transport was analyzed using two-photon luminescence (TPL) imaging, computed tomography (CT), and radio-labelling. These findings validate the viability of implementing the developed multifunctional GNSs for in vivo tracking at different goal scales and for image-guided PTT in the treatment of malignant development. Adjustments to reaction conditions, such as pH, will cause a shift in equilibrium circumstances during Ag and Au synthesis.

## 2. LITERATURE REVIEW

Xia, X. R., Monteiro-Riviere, N. A. et al,(2010) The molecular interactions between chemical groups on the nanoparticle surfaces and the amino-acid residues of the proteins govern the selective absorption of proteins by nanoparticles in a physiological environment, resulting in 'nanoparticle-protein coronas. To quantify the competitive adsorption of a set of small molecule probes onto the nanoparticles and thus characterize these interactions, we propose a biological surface adsorption index. It is generally believed that Coulomb forces, London dispersion, hydrogen-bond acidity and basicity, polarizability, and lone-pair electrons govern the adsorption properties of nanomaterials. The probe compounds' adsorption coefficients were measured, and these data were used to generate

a set of nanodescriptors that account for the various factors and strengths of the molecular interactions. The method was able to accurately predict the adsorption of a wide range of small molecules onto carbon nanotubes, and the nanodescriptors were also successfully measured for a further 12 nanomaterials. Nanodescriptors based on the biological surface adsorption index can be used to create models for assessing the pharmacokinetics and safety of nanomaterials.

Baer, D. R., Engelhard, M. H. et al,(2013) The difficulties in characterizing nanomaterials and the ways in which surface and interface characterization techniques can help address these difficulties are discussed in this review. There is a growing awareness in certain sectors of the academic community that characterization of nanomaterials in published studies and reports is often inadequate or incomplete. In light of this, it is difficult to know how reliable the information contained in such reports really is. Given the growing importance of nanomaterials in both basic and applied research, it is important that scientists from all the different fields working with them understand the nature of the unexpected challenges they face when trying to synthesize and characterize nanomaterials in a way that can be replicated. Extending the methods of conventional data analysis can often provide many more insights than are apparent at first glance.

Sayes, C. M., & Warheit, D. B. (2009) A thorough physicochemical characterisation of the test material under study is a vital component of any strategy for screening nanomaterial toxicity. Essential for comparing toxicity data with the hazard-based findings of other investigators and for linking the nanoparticle surface properties with any measurable biological/toxicological responses. In addition, it is crucial to guarantee that the nanoparticle-types are identical or very similar in composition when hazard or risk-based evaluations are made on a specific nanomaterial (based on a number of studies). Achieving this goal requires intensive characterisation efforts. Nanoparticle-types with similar chemical compositions may have different sizes, shapes, crystal structures, surface coatings, and surface reactivity characteristics, making it easy to draw broad conclusions



without conducting a thorough analysis of the physical characteristics. Since the fate, accumulation, and transport of nanomaterials through the body over time may be predicted based on specific surface characteristics, determining nanomaterial physicochemical properties is crucial to nano medicinal applications.

Sadik, O. A., Du, N., Kariuki, V. et al, (2014) In one dimension, engineered nanoparticles (ENPs) are extremely small, typically between 1 and 100 nm. When compared to a bulk solid or dissolved substance of the same composition, ENPs behave considerably differently due to their small size and huge surface areas relative to their weight. Their mechanical, magnetic, catalytic, electrical, optical, and biological properties can thus be easily altered. ENPs are increasingly useful materials for applications in a wide variety of industries, such as food additives, cosmetics, biological samples, medicines, biocide packaging, fuel cell technology, and electronics. However, worries about ENPs' long-term persistence in the environment, potential toxicity, and overall dangers to environmental and human health have grown in tandem with their increased use in consumer items. Therefore, it is crucial to create analytical tools and methodologies that are particularly helpful for assessing ENPs in complex matrices, consumer goods, and consumer electronics. The ideal instruments will be adaptable to the unique characteristics of ENPs, including particle size, particle number, and mass. These techniques should be flexible enough to assess the NPs' size, dispersion, and toxicity in addition to their mass concentration.

Liu, C. J., Burghaus, U. et al, (2010) When it comes to processing fuels from fossil fuel resources like coal, petroleum, and natural gas, nanotechnology has played a crucial role in the design, synthesis, and characterisation of a wide range of new and revolutionary energy materials and catalysts. 90% of the world's energy consumption still comes from fossil fuels, and that number is predicted to peak around 2050. Problems arise when people rely too heavily on fossil fuels, such as the fact that they cause climate change and that there won't be enough crude oil to go around in the long run. This is why research into renewable energy and energy storage technologies is crucial. We may expect nanoscience and

nanotechnology to play substantially larger roles in the years to come. Breakthroughs in a variety of sustainable energy technologies depend critically on the synthesis and characterisation of new and unique functional nanomaterials with highly regulated sizes, shapes, porosities, crystalline phases, and topologies. In spite of this, for the next two to four decades, fossil fuels will likely continue to be the world's dominant energy source. Accordingly, new catalysts are needed to manage shifts in the fossil fuel supply and to address the resulting environmental issues.

Ikhmayies, S. J. (2014) Since nanomaterials have features that set them apart from bulk solids and molecules, they have garnered a lot of interest. Quantum phenomena have a role in the unique size-dependent characteristics of nanomaterials in the 1–100 nm range. As the particle's radius gets closer to the asymptotic exciton Bohr radius, quantum confinement starts to show its effects. As a result of their high surface-to-volume ratio, surface properties have a profound impact on nanomaterials' underlying structures, which is one of the reasons for their unique characteristics. Nanomaterials are the subject of extensive study for their potential use in a wide range of fields and industries, including energy storage and conversion, solar cells, pharmaceuticals, life science applications, optoelectronics, sensing and actuation nanosystems, catalysis, and composite materials. Nanomaterials can be characterized using a wide variety of methods, such as electron microscopy, scanning probe microscopies in particular, atomic force microscopy, x-ray diffraction, neutron diffraction, x-ray scattering, x-ray fluorescence spectrometry, the acoustic wave technique, contact angle measurements, and various spectroscopies.

### 3. RESEARCH METHODOLOGY

#### METHODOLOGY

Because of its efficiency, simplicity, and cheap cost, the hydrothermal synthesis process may very well be the favoured option. Sir Roderick Murchison (1792–1871), an English geologist, was the first to adopt the term "hydrothermal" to describe the process by which the tremendous pressure of water molecules at high temperatures leads to the production of rocks



and minerals in the earth's crust. The first hydrothermal technique to create carbonates of Ba (barium) and Sr was reported by R. W. Bunsen in 1839. (strontium). Roy and Tuttle provided a thorough study for the use of this approach in 1956. In the period between 1950 and 1970, Roy et al. generated a wide variety of clay minerals and different zeolite compositions utilising the hydrothermal technique. The hydrothermal approach received a lot of interest when new high resolution microscopy tools were available in the late 1980s for the development of materials in the nanoscale domain. Since then, several other multifunctional materials have been created using the hydrothermal process.

### 3.2 Production Methods of Nanomaterials

#### 3.2.1. Approaches for the Preparation of Nanomaterials

Synthesis of nanomaterials and production of nanostructures can be accomplished using one of two methods. Using techniques like attrition and milling, top-down methods involve gradually reducing a bulk material to particles on the nanoscale through slicing or successive cutting. Bottom-up procedures are those in which components assemble themselves. The process is best illustrated by chemical reactions (see Figure 3). While the bottom-up method is commonly used in the parallel production of devices and is more cost-effective than top-down approaches, it can be difficult to manage the techniques when the products become larger and more cumbersome than what is typically produced by substance union. Molding, carving, and cutting are just a few examples of the widespread methods used in the partial manufacture of available biomedical supplies. The difficulties inherent in these methods mean that very sophisticated nanotools have not yet been created.

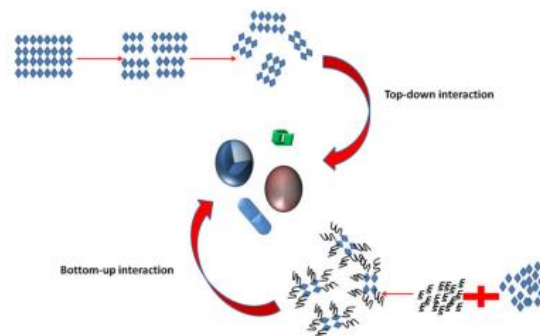


Figure 3. Diagram demonstrating the difference between top-down and bottom-up theories.

#### 3.2.2. Inorganic NPs

Since inorganic NPs can serve as viable replacements for conventional anti-cancer and antibacterial medications, this fact has stoked renewed interest in their application in the pharmaceutical sector. In response to these developments, pharmaceutical companies focused on the creation of unconventional medicines, and in particular nanotechnology businesses, have renewed their commitment to the research and development of novel nanomaterials that have been identified as promising operators against bacteria and cancer cells that have become resistant to conventional antibiotics and anti-cancer drugs.

#### Chemical Precipitation

Due to its low cost and ease of use, the chemical precipitation method is widely used in the production of a wide variety of nanomaterials with potential medical applications. The primary difficulties in this technique stem from the necessity of preventing the formation of physical changes in the preparation medium and the aggregation of small crystallites throughout the synthesis operation. To regulate thermal coagulation and Oswald ripening, double-layer repulsion is induced by using non-aqueous solvents at lower temperatures. The dopant materials should be added before the precipitation in this procedure, and the reaction should take place in a solvent that is compatible with all the reactants. As an added measure, the use of certain surfactants can be implemented to stop the NPs from clumping together. Once the NPs have been collected, washed, and dried (by means of centrifugation equipment and an oven, respectively), they can be used. It can be helpful to use ultraviolet light to polymerize the



surfactant layer that caps the NPs, thereby preserving their original sizes. Previous research has highlighted how different surfactant types can affect the final properties of NPs, which in turn can be used to regulate their applications.

### Sol-Gel Technique

Since their inception, NPs for use in medicine have been prepared using the sol-gel processing method. It is well known that when dispersed in aqueous solvents, NPs or normal molecules make clear solutions while colloidal particles produce a cloudy one. The basic idea behind this procedure is that the initial colloidal suspensions will eventually solidify into a continuous liquid-phase network (gel) (sol). They are complexes of metal alkoxide ions with aloxysilanes. Sol-gel processes typically begin with the alkoxides tetramethoxysilane (TMOS) and tetraethoxysilanes (TEOS), which, due to their immiscibility in water, react to form silica gels. Alcohols are utilized as mutual solvents in the synthesis of these organometallic precursors for a wide variety of metals such as silicon, aluminum, titanium, zirconium, and many more. To get consistent nanomaterials, the sol-gel method needs to incorporate at least one of the selected alkoxides. Because of its low-cost starting materials, simple preparation stages, and simple scale-up manufacturing techniques, the chemical precipitation technique outperforms the sol-gel technique in practice.

### Nanopolymers

When deciding on a suitable method for the formation of NPs, it is important to consider the physicochemical properties of both the polymer and the drug. Materials including proteins, polysaccharides, and man-made polymers can all be used in the creation of NPs. There are a lot of factors to consider when deciding what kind of

grid material to use, and they're all shown out in Figure 4.

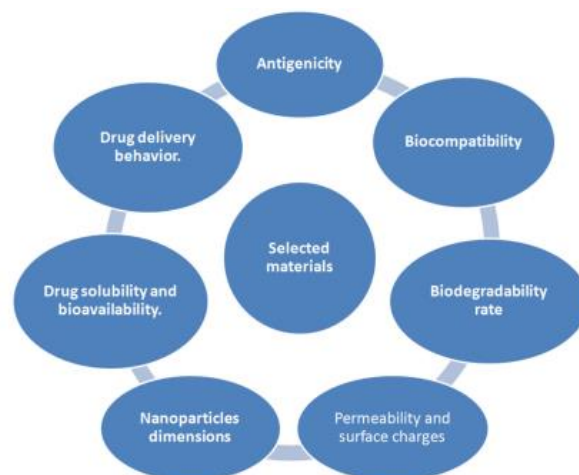
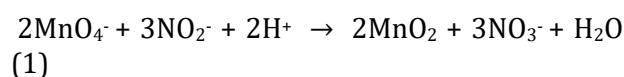


Figure 4. Key elements that should be considered while selecting nanomaterials for biomedical field.

## 4. RESULTS AND DISCUSSION

### Morphology and phase analyses

During the hydrothermal reaction, hydrothermal pressure and H<sup>+</sup> ions play a crucial role in morphological changes as well as phase transition of MnO<sub>2</sub>. The extreme hydrothermal pressure forces reactants molecules to appear in ionic forms as described below:



Here, permanganate ion acts as an oxidant and resource of manganese (Mn) element, whereas nitrite ions are used as a reducing agent. It is conspicuous that the stoichiometric molar ratio of permanganate to nitrite ions is 2 : 3. For proper feasibility of the hydrothermal reaction, potassium permanganate and sodium nitrate precursors are utilized in the molar



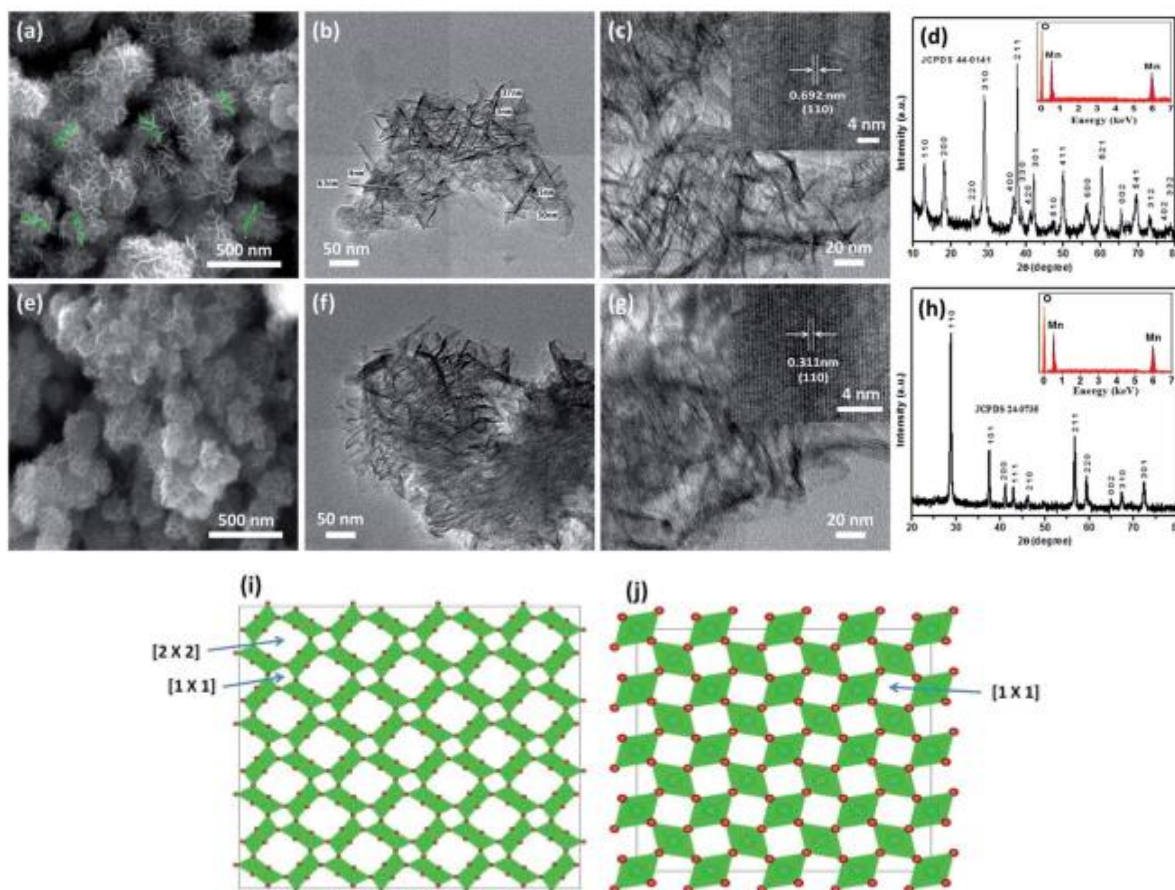


Fig. 5 (a) FESEM image, (b and c) HRTEM image with (inset c) d-spacing  $\frac{1}{4}$  0.692 nm in growth direction (110) and (d) XRD pattern with (inset d).

Involvement of protons is crucial for the reaction to be possible, as stated by Le Chatelier's principle. Sulphuric acid provides the reacting protons ( $H^+$  ions). Variations in the product's form, size, and phase can result from changes in the concentration of  $H^+$  ions. According to the Nernst equation, when the concentration of hydrogen ions ( $H^+$ ) rises, the reducing power of permanganate ions falls. As the reduction potential of permanganate ions decreases, the reduction potential of nitrite ions rises to achieve equilibrium, which in turn accounts for a higher production rate of  $Mn^{4+}$  ions. Since  $H^+$  ions directly regulate  $Mn^{4+}$  levels in our system, this is the case. The construction of a more modest outlook for as synthesized material was made possible by lowering the acidic content, which in turn lowered the  $Mn^{4+}$  concentration or growth unit [ $MnO_6$ ]. Sample S1, generated with 0.2 mL  $H_2SO_4$ , exhibits nanostructures, as seen in FESEM (Fig. 5a) and HRTEM (Figs. 5b and 5c). Nanocacti-like shape can be seen in visible nanostructures, which are composed of

nanowires with diameters between 1 and 10 nm and which self-assemble from ultrathin sheets. Sample S1 has a 0.692 nm d-spacing along the direction of growth (Fig. 5c inset). This suggests a phase of the material, which is corroborated by the XRD study. Major diffraction peaks at  $2\theta$  14.12.7, 18.1, 28.8, 37.4, 49.8, and 60.2 can be seen in the XRD pattern of the sample S1 (Fig. 5d) synthesized with 0.2 mL  $H_2SO_4$ . These peaks correspond to the tetragonal phase of  $\alpha$ - $MnO_2$  (JCPDS 44- 0141). Additionally, XRD patterns show that any newly formed  $\alpha$ - $MnO_2$  crystals tend to expand in a horizontal plane. Sample S1's EDS pattern is shown in the inset of Fig. 5d. The absence of impurity peaks indicates that the as prepared sample is pure.

There was no discernible morphological change even when the acid concentration was raised to 0.3 mL. Sample S2, prepared with 0.3 mL of  $H_2SO_4$ , displays almost identical morphology to sample S1 in FESEM (Fig. 5e) and HRTEM (Figs. 5f and 5g) images. In the (110) growth direction, the observed d-spacing was 0.311 nm, as

depicted in the inset of Fig. 5g. However, in our system, the enhancement of Mn<sup>4+</sup> ions caused by an increase in H<sup>+</sup> ions concentration causes the material to undergo a phase transition. Sample S2's XRD patterns (Fig. 5h) exhibit three prominent diffraction peaks at 2θ 14 28.68, 37.33, and 56.65, all of which are consistent with

the tetragonal phase of b-MnO<sub>2</sub>. After that, b-MnO<sub>2</sub> crystals form, and they preferentially expand in the (110) direction. Pure b-MnO<sub>2</sub> nanocacti were obtained, as evidenced by the absence of any peaks corresponding to impurities and the presence of sharp peaks for the elements manganese and oxygen.

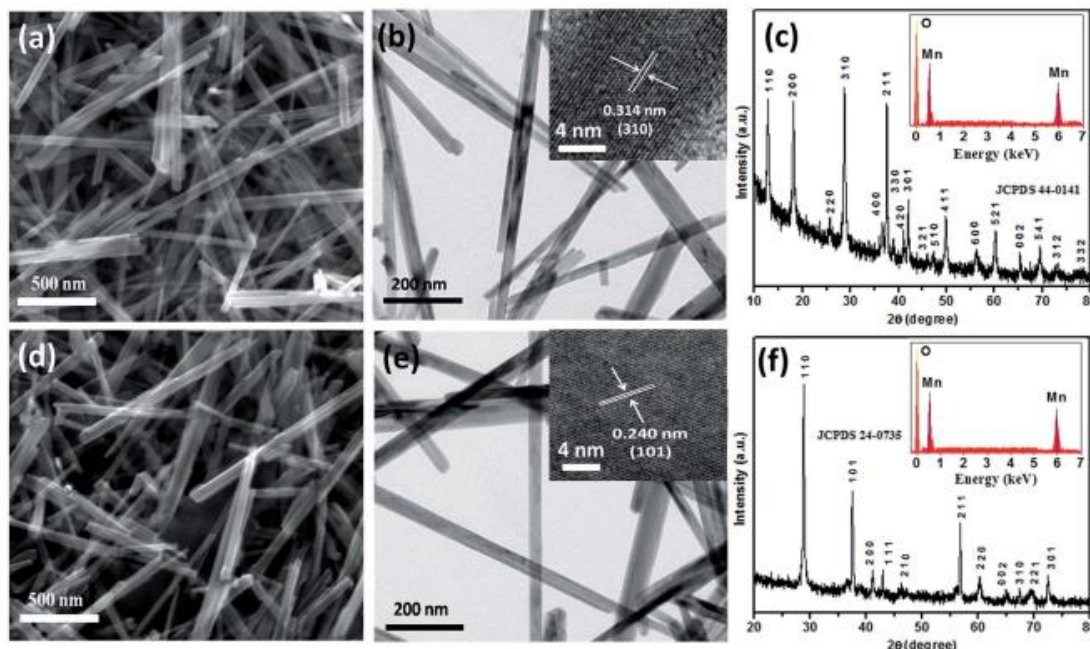
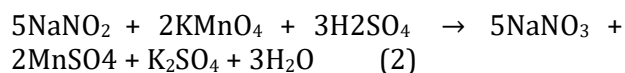


Fig. 6 (a) FESEM image, (b) HRTEM image with (inset b) d-spacing ¼ 0.314 nm in growth direction.

Sample S3, produced in 0.3 M H<sub>2</sub>SO<sub>4</sub>, has a morphology resembling 1D nanorods with diameters between 10 and 40 nm, as seen in FESEM (Fig. 6a) and HRTEM (Fig. 6b). It is clear from the XRD pattern in Fig. 6c that the MnO<sub>2</sub> nanorods are a-phase, as suggested by their d-spacing of 0.314 nm and the growth direction (310) indicated in the inset. Tetragonal phase of a-MnO<sub>2</sub> can be identified from the diffraction peaks (JCPDS card number 44-0141). The EDS pattern seen in the inset of Fig. 6c excludes the presence of any contaminants and further suggests for high purity of the as prepared sample. Nanorods, rather than nanocacti, form when H<sub>2</sub>SO<sub>4</sub> is added to the reacting solution drop by drop from a 0.3-0.4 M H<sub>2</sub>SO<sub>4</sub> solution, as opposed to 0.2-0.3 mL of concentrated H<sub>2</sub>SO<sub>4</sub> added all at once. In this way, the optimal concentration of reactants may be anticipated before to initiating the hydrothermal process, allowing for the prediction of both the product's phase and morphology. The following reaction, which is hypothesized to take place before the

hydrothermal process, may provide a better explanation.



The formation of 1D nanorods demonstrates that there is a critical window of time during which every chemical process can be carried out successfully.

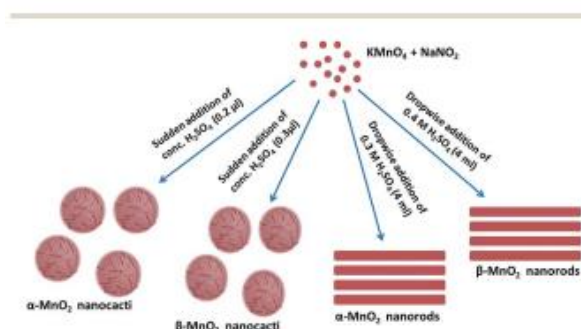


Fig. 7 Schematic showing the formation of a- and b-MnO<sub>2</sub> nanocacti and a- and b-MnO<sub>2</sub> nanorods at different reaction conditions.

Addition of H<sub>2</sub>SO<sub>4</sub> abruptly completes the beginning requirements of the aforementioned



reaction, resulting to the synthesis of  $MnSO_4$  compound, and makes manganese ions available as  $Mn^{2+}$  rather than  $Mn^{4+}$ . Fortunately, the above reaction can be slowed down by adding  $H_2SO_4$  drop by drop, as the lack of  $SO_4^{2-}$  actually works in favor of the presence of  $Mn^{4+}$  ions. Therefore, 1D morphologies (nanorods) with larger diameters of 10-40 nm are visible when an adequate amount of  $Mn^{4+}$  ions are present as stabilizers, in contrast to the narrower 1D morphologies (nanowires with diameters in the range of 1-10 nm) observed in nanocacti. Similar nanorods also existed when the acid content was raised to 0.4 M  $H_2SO_4$ . Sample S4, which was produced in 0.4 M  $H_2SO_4$ , has 1D morphologies with diameters in the 10- to 40-nm range, as seen in both FESEM (Fig. 7d) and HRTEM (Fig. 7e). Phase changes are an obvious result of a rise in acid content. Based on the XRD pattern and the reported d-spacing of 0.24 nm in the growth direction (101) for sample S4, b-phase can be assigned (Fig. 7f). Major diffraction peaks in sample S4's XRD patterns match those predicted for the tetragonal phase of b- $MnO_2$  (JCPDS card

number 24-0735). The absence of impurity peaks in the respective EDS pattern displayed in the inset of Fig. 7f attests to the high purity of the as prepared sample S4. The transition from the a- to the b-phase can be explained by the fact that the  $H^+$  concentration increases along with the molar concentration of  $H_2SO_4$  from 0.3 M to 0.4 M. Nanorods and nanocacti both showed a b phase stability at a pH value of 2, while at a relatively weak acidity of 4 pH, a phase stability was observed for both morphologies. We see the phase and morphological changes that occur during the synthesis of  $MnO_2$  nanostructures at varying acid counts. Further research is needed to determine the precise reasons behind  $MnO_2$ 's phase and morphological changes.

Growth process of a- $MnO_2$  nanocacti is monitored through FESEM analysis when the hydrothermal process was carried out at different time intervals of 4, 8 and 12 h (Fig. 8a-c, respectively) using 0.2 mL  $H_2SO_4$ . The growth process starts with nucleation,

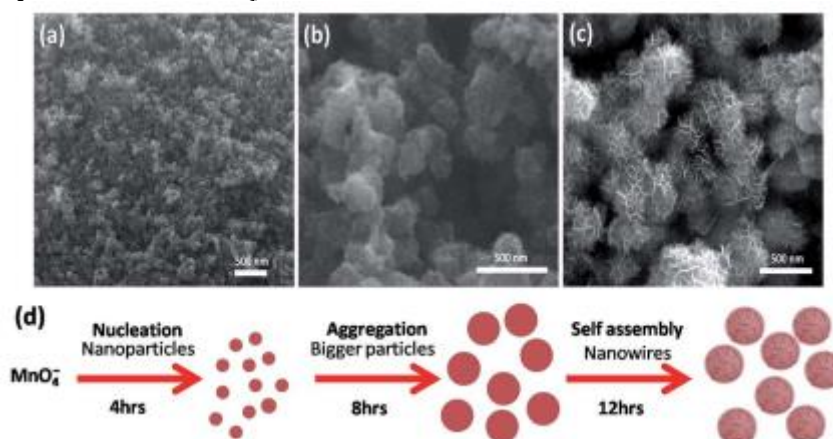


Fig. 8 (a-c) FESEM images taken after 4, 8 and 12 h, respectively during the synthesis of sample S1 using 0.2 mL of  $H_2SO_4$ . (d) Schematic of a- $MnO_2$  nanocacti growth process.

when the rate at which  $MnO_4^-$  ions undergo redox reaction to create  $MnO_2$  is significantly boosted during the first stage of the hydrothermal process. After 4 hours of reaction time, nanoparticles are formed as the supersaturated nuclei clump together, lowering the interfacial energy (Fig. 8a). when the reaction time was increased to 8 hours, the nanoparticles aggregated by growing larger in order to reduce the interfacial energy. By 12 hours, the molecules of the reactants had stabilized enough to form

nanowires, which built themselves from ultrathin sheets (Fig. 8c).

## CONCLUSION

In light of the aforementioned points, a number of review publications have covered the essential elements of nanomaterial design from various points. They include drug formulations for specific populations (such as pediatric applications), global assessments of nanotechnology, the state of nanorobotics in

medicine, specific nanomaterial applications (such as antioxidants for cancer treatment), nanomaterial incorporation in bioimaging technologies, skin-contact nanoelectrodes, subcellular nanodevices, and others. In contrast, there is a general lack of critical review that specifically disseminates the relevant knowledge for the design of NP shapes and sizes, as well as their synthesis methodologies and characterisation techniques for commercial biomedical applications, i.e., outside of the typical small-scale laboratory experiments.

The multiple difficulties involved in the commercial-scale (bulk) production of nanomaterials for biological applications are what we blame for this gap in the conversation. One of these difficulties is figuring out how to produce nanomaterials in big quantities at a low cost, which necessitates defining a preparatory production that can be scaled up sufficiently to pay the cost necessary for targeting volume markets. The above-mentioned aspects must be taken into consideration when supplying the nanomaterials in a specific structure for inclusion in the assembly form.

It's interesting that the behavior of NPs' surface and how these particles can be dispersed in a wide range of media are crucial, and this behavior can be influenced by changing the design parameters of the NPs. For straightforward compounds like oxides of NPs, it is occasionally possible to achieve NPs' consistent size and the unwavering quality of their chemical compositions; however, achieving this for a staggering number of materials in volume manufacture is not simple. It is possible to describe materials to a remarkable degree through the characterization of nanoparticles. A large number of procedures are suitable for laboratory testing but not for use in a production setting. To screen features like particle size, quick, efficient, and mass techniques are needed. The current review, which introduces thorough information on these factors, is urgently needed, according to all of the above.

These unique properties of nanoparticles, including biological, chemical, electrical, magnetic, optical and physical properties, differ greatly from the same materials in their bulk form. For examples, nanomaterials offer enhanced Raman and Rayleigh scattering

properties in metal NPs (such as gold and silver), supermagnetic properties in magnetic materials and a quantum effect in semiconductors. Such NPs form the next generation building blocks for biomedical, chemical, electronic and optical applications. In recent years, nanoparticles have also found applications in the environmental, petroleum, food and textile industries. Whereas, in the past metal nanoparticles such as gold and silver were studied in great detail, the last decade has seen the rise in research of other metal nanoparticles such as copper, palladium, platinum and various metal oxides.

## REFERENCES

1. Ashraf, W., Fatima, T., Srivastava, K., & Khanuja, M. (2019). Superior photocatalytic activity of tungsten disulfide nanostructures: role of morphology and defects. *Applied Nanoscience*, 9(7), 1515-1529.
2. Xue, M. Q., Tang, H., & Li, C. S. (2015). Synthesis and tribological properties of TiC micro and nanoparticles. *International Journal of Surface Science and Engineering*, 9(1), 69-80.
3. Ajibade, P. A., Sikakane, B. M., Botha, N. L., Oluwalana, A. E., & Omondi, B. (2020). Synthesis and crystal structures of bis (dibenzyl dithiocarbamate) Cu (II) and Ag (I) complexes: Precursors for Cu<sub>1</sub> 8S and Ag<sub>2</sub>S nano-photocatalysts. *Journal of Molecular Structure*, 1221, 128791.
4. Lin, S., Liu, L., Hu, J., Liang, Y., & Cui, W. (2015). Nano Ag@ AgBr surface-sensitized Bi<sub>2</sub>WO<sub>6</sub> photocatalyst: oil-in-water synthesis and enhanced photocatalytic degradation. *Applied Surface Science*, 324, 20-29.
5. Zhao, J., Han, Q., Zhu, J., Wu, X., & Wang, X. (2014). Synthesis of Bi nanowire networks and their superior photocatalytic activity for Cr (VI) reduction. *Nanoscale*, 6(17), 10062-10070.
6. Barka-Bouaifel, F., Sieber, B., Bezzi, N., Benner, J., Roussel, P., Boussekey, L., ... & Boukherroub, R. (2011). Synthesis and photocatalytic activity of iodine-doped



- ZnO nanoflowers. *Journal of Materials Chemistry*, 21(29), 10982-10989.
7. Sirota, B., Reyes-Cuellar, J., Kohli, P., Wang, L., McCarroll, M. E., & Aouadi, S. M. (2012). Bismuth oxide photocatalytic nanostructures produced by magnetron sputtering deposition. *Thin Solid Films*, 520(19), 6118-6123.
  8. Hu, K. H., Liu, Z., Huang, F., Hu, X. G., & Han, C. L. (2010). Synthesis and photocatalytic properties of nano-MoS<sub>2</sub>/kaolin composite. *Chemical Engineering Journal*, 162(2), 836-843.
  9. Lin, P. C., Lin, S., Wang, P. C., & Sridhar, R. (2014). Techniques for physicochemical characterization of nanomaterials. *Biotechnology advances*, 32(4), 711-726.
  10. Xia, X. R., Monteiro-Riviere, N. A., & Riviere, J. E. (2010). An index for characterization of nanomaterials in biological systems. *Nature nanotechnology*, 5(9), 671-675.
  11. Baer, D. R., Engelhard, M. H., Johnson, G. E., Laskin, J., Lai, J., Mueller, K., ... & Moon, D. (2013). Surface characterization of nanomaterials and nanoparticles: Important needs and challenging opportunities. *Journal of Vacuum Science & Technology A: Vacuum, Surfaces, and Films*, 31(5), 050820.

